Remarkable reversal of melting point alternation by co-crystallization

Dario Braga,* Elena Dichiarante, Giuseppe Palladino, Fabrizia Grepioni,* Michele R. Chierotti, Roberto Gobetto* and Luca Pellegrino

ESI
Electronic Supplementary Material
(21 pages)

Legenda

1C4 = bpa:succinic acid

1C5 = bpa:glutaric acid

1C6 = bpa:adipic acid

1C7 = bpa:pimelic acid

1C8 = bpa:suberic acid

1C9 = bpa:azelaic acid

1C10 = bpa:sebacic acid

2C4 = bpp:succinic acid (CSD refcode = **JAZBES**)

2C5 = bpp:glutaric acid

2C6 = bpp:adipic acid

2C7 = bpp:pimelic acid

2C8 = bpp:suberic acid

2C9 = bpp:azelaic acid

2C10 = bpp:sebacicacid

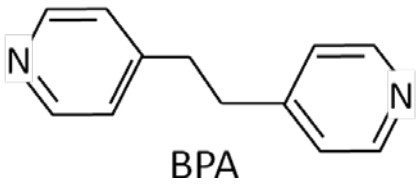

BPA

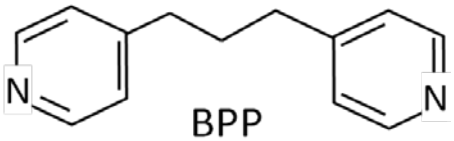

BPP

EXPERIMENTAL

All reactants were purchased from Aldrich and used without further purification. Reagent grade solvents and doubly-distilled water were used. In all cases, correspondence between the structure of the solid residue and that obtained by single-crystal X-ray diffraction was ascertained by comparing measured X-ray powder diffractograms with those calculated on the basis of single-crystal data.

Solution syntheses of 1·C_n (n = 4-10)

*Solution synthesis of **1· C4**:*
Single crystals of ***1·C4*** suitable for single crystal X-ray diffraction were obtained by slow evaporation of a solution obtained dissolving **1** (0.1890 mg, 1.0258 mmol) and Succinic acid $HOOC(CH_2)_2COOH$, (0.1211 g, 1.0255 mmol) in hot methanol 99.8%.

*Solution synthesis of **1·C5**:*
Single crystals of ***1·C5*** suitable for single crystal X-ray diffraction were obtained by slow evaporation of a solution obtained dissolving **1** (0.1868 mg, 1.0138 mmol) and Glutaric acid $HOOC(CH_2)_3COOH$, (0.1329 g, 1.006 mmol) in hot methanol 99.8%.

*Solution synthesis of **1·C6**:*
Single crystals of ***1·C6*** suitable for single crystal X-ray diffraction were obtained by slow evaporation of a solution obtained dissolving **1** (0.1235 mg, 0.6703 mmol) and Adipic acid $HOOC(CH_2)_4COOH$, (0.0984 g, 0.6733 mmol) in hot methanol 99.8%.

*Solution synthesis of **1·C7**:*
Single crystals of ***1·C7*** suitable for single crystal X-ray diffraction were obtained by slow evaporation of a solution obtained dissolving **1** (0.2138 mg, 1.1604 mmol) and Pimelic acid $HOOC(CH_2)_5COOH$, (0.1860 g, 1.1613 mmol) in hot methanol 99.8%.

*Solution synthesis of **1·C8**:*
Single crystals of ***1·C8*** suitable for single crystal X-ray diffraction were obtained by slow evaporation of a solution obtained dissolving **1** (0.2008 mg, 1.0898 mmol) and Suberic acid $HOOC(CH_2)_6COOH$, (0.1890 g, 1.0850 mmol) in hot methanol 99.8%.

*Solution synthesis of **1·C9**:*
Single crystals of ***1·C9*** suitable for single crystal X-ray diffraction were obtained by slow evaporation of a solution obtained dissolving **1** (0.1854 mg, 1.006 mmol) and Azelaic acid $HOOC(CH_2)_7COOH$, (0.1889 g, 1.004 mmol) in hot methanol 99.8%.

*Solution synthesis of **1·C10**:*
Single crystals of ***1·C10*** suitable for single crystal X-ray diffraction were obtained by slow evaporation of a solution obtained dissolving 1 (0.1604 mg, 0.8728 mmol) and Sebacic acid $HOOC(CH_2)_8COOH$, (0.1759 g, 0.8697 mmol) in hot methanol 99.8%.

Solution syntheses of 2·C_n (n = 4-10)

*Solution synthesis of **2·C4** (CSD refcode = **JAZBES**):*
Crystalline powder for X-ray diffraction, DSC and SSNMR was obtained by evaporation of a solution prepared dissolving 4,4'-Trimethylenedipyridine (0.1059g,0.534mmol) and succinic acid $HOOC(CH2)_2COOH$, (0.0631g, 0.534mmol) in hot methanol.

*Solution synthesis of **2·C5**:*
Single crystals of Glutaric Acid: 4,4'-Trimethylenedipyridine suitable for single crystal X-ray diffraction were obtained by slow evaporation at 4°C of a solution obtained dissolving 4,4'-Trimethylenedipyridine (0.09g, 0.457mmol) and Glutaric acid $HOOC(CH2)_3$ COOH, (0.0604g, 0.457mmol) in hot methanol.

*Solution synthesis of **2·C6**:*
Single crystals of Adipic Acid: 4,4'-Trimethylenedipyridine suitable for single crystal X-ray diffraction were obtained by slow evaporation at 4°C of a solution obtained dissolving 4,4'-Trimethylenedipyridine (0.127g, 0.642mmol) and Adipic acid $HOOC(CH2)_4$ COOH, (0.095g, 0.642mmol) in hot water.

*Solution synthesis of **2·C7**:*
Single crystals of Pimelic Acid: 4,4'-Trimethylenedipyridine suitable for single crystal X-ray diffraction were obtained by slow evaporation at 4°C of a solution obtained dissolving 4,4'-Trimethylenedipyridine (0.0862g, 0.435mmol) and Pimelic acid $HOOC(CH2)_5$ COOH, (0.0696g, 0.435mmol) in hot methanol.

*Solution synthesis of **2·C8**:*
Single crystals of Suberic Acid: 4,4'-Trimethylenedipyridine suitable for single crystal X-ray diffraction were obtained by slow evaporation at 4°C of a solution obtained dissolving 4,4'-Trimethylenedipyridine (0.176g, 0.886mmol) and Suberic acid $HOOC(CH2)_6$ COOH, (0.155g, 0.886mmol) in hot methanol.

*Solution synthesis of **2·C9**:*
Single crystals of Azelaic Acid: 4,4'-Trimethylenedipyridine suitable for single crystal X-ray diffraction were obtained by slow evaporation at 4°C of a solution obtained dissolving 4,4'-Trimethylenedipyridine (0.053g, 0.269mmol) and Azelaic acid $HOOC(CH2)_7$ COOH, (0.051g, 0.269mmol) in hot methanol.

*Solution synthesis of **2·C10**:*
Single crystals of Sebacic Acid: 4,4'-Trimethylenedipyridine suitable for single crystal X-ray diffraction were obtained by slow evaporation at 4°C of a solution obtained dissolving 4,4'-Trimethylenedipyridine (0.065g, 0.329mmol) and Sebacic acid $HOOC(CH2)_8$ COOH, (0.068g, 0.329mmol) in hot methanol.

Crystal structure determination

Single-crystal data for all compounds were collected on an Oxford X'Calibur S CCD diffractometer equipped with a graphite monochromator (MoKα radiation, λ = 0.71073) and operated at room temperature. were collected at RT on an X'calibur S, Oxford Diffraction. Crystal data and details of measurements are summarised in ESI-XRAY Table 1 and ESI-XRAY Table 2. SHELX97[1a] was used for structure solution and refinement based on F^2. All non-hydrogen atoms were refined anisotropically. PLATON[1b] was used for hydrogen bonding analysis, and SCHAKAL99[1c] was used for the graphical representation of the results. X-ray powder diffractograms were collected on a Panalytical X'Pert PRO automated diffractometer equipped with an X'Celerator detector. A Cu anode was used as X-ray source at 40KV and 40 mA. The program PowderCell 2.2[1d] was used for calculation of the X-ray powder patterns.

1 (a) G. M. Sheldrick, *SHELX97, Program for Crystal Structure Determination*; University of Göttingen: Göttingen, Germany, 1997; (b) A. L. Speck, PLATON; *Acta Crystallogr*., *Sect*. *A*, 1990, 46, C34. (c) E. Keller, SCHAKAL99, Graphical Representation of Molecular Models, University of Freiburg, Germany, 1999; (d) PowderCell programmed by W. Kraus and G. Nolze (BAM Berlin) © subgroups derived by Ulrich Müller (Gh Kassel).

ORTEP DRAWINGS FOR ALL COMPOUNDS

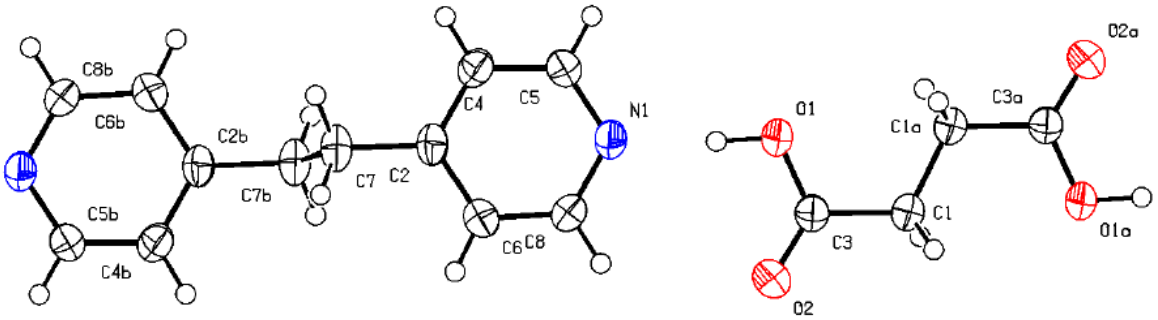

1·C4

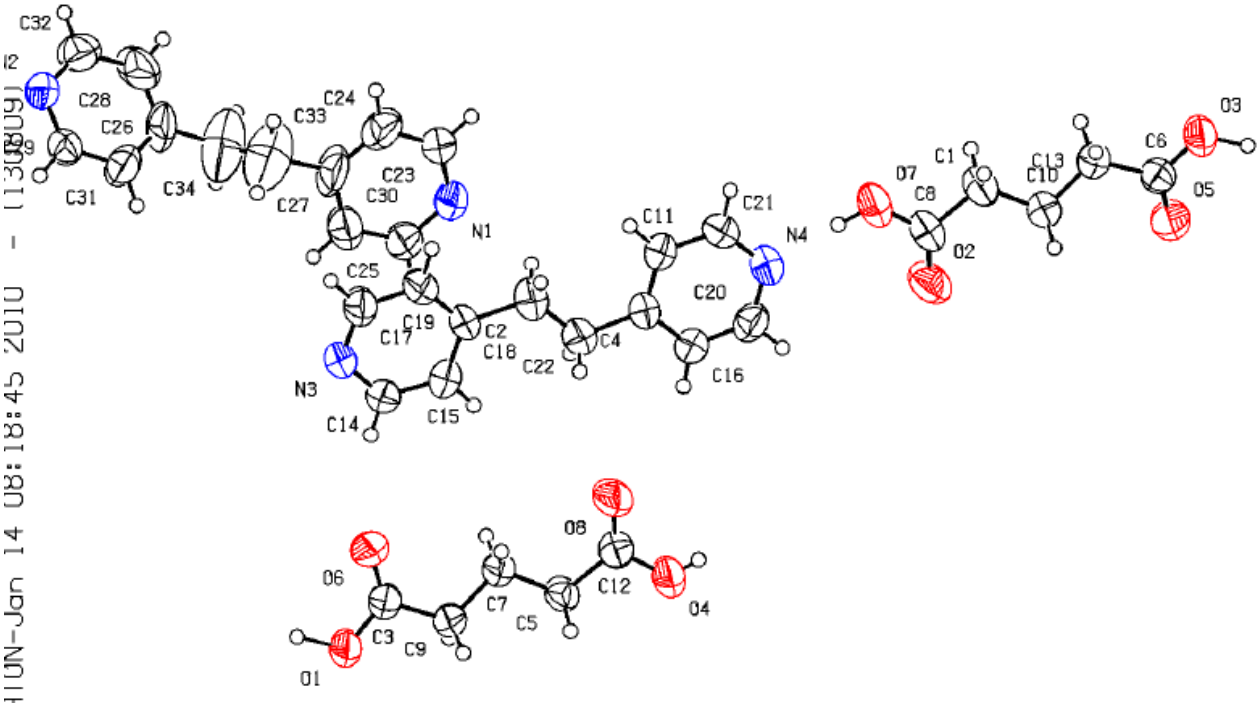

1·C5

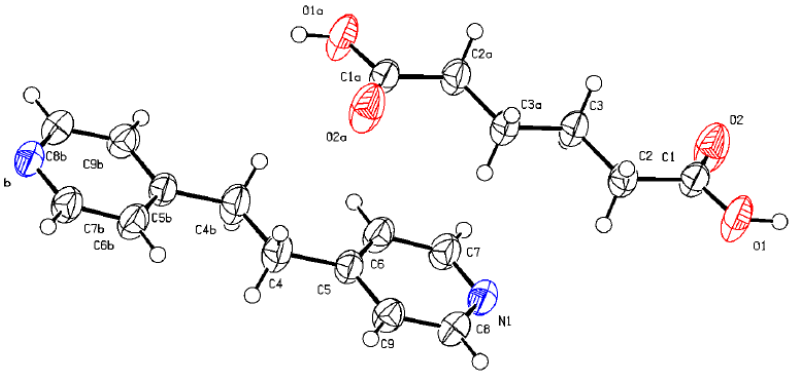

1·C6

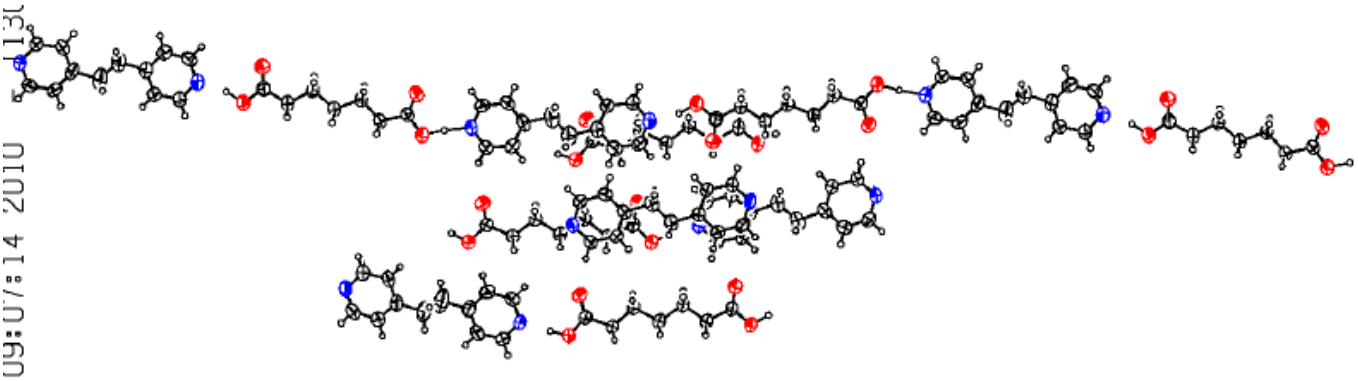

1·C7

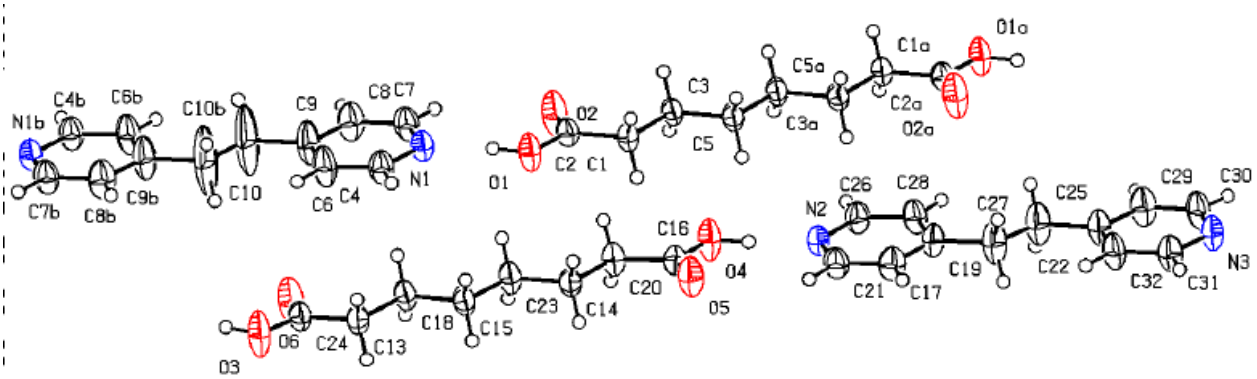

1·C8

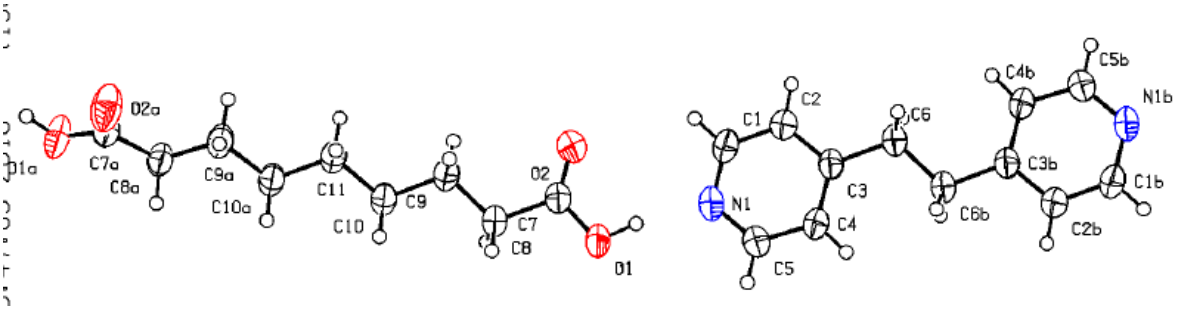

1·C9

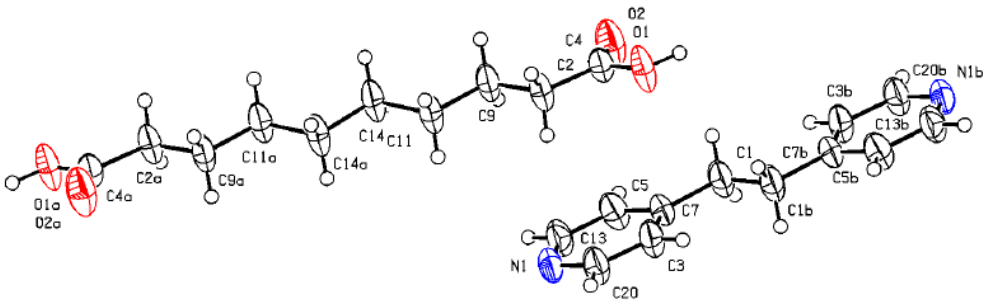

1·C10

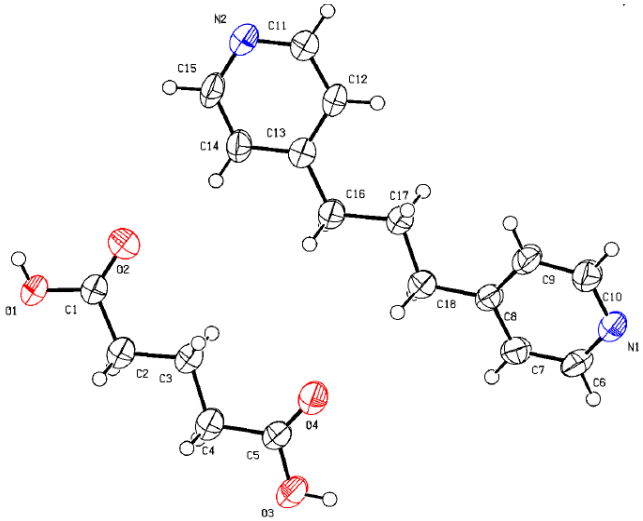

2·C5

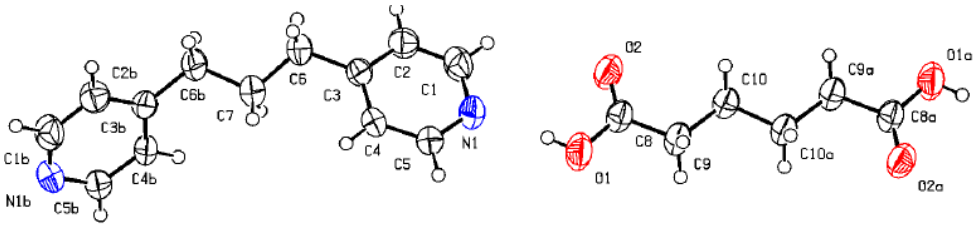

2·C6

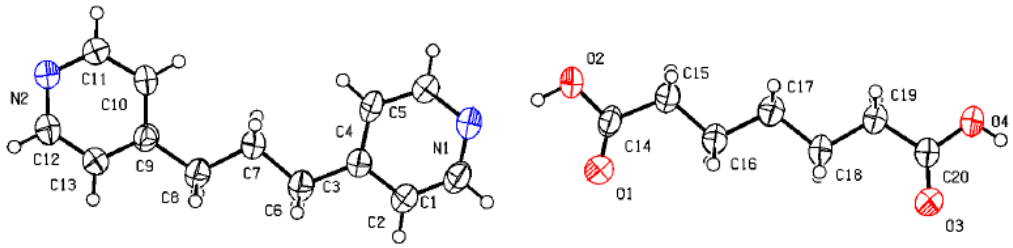

2·C7

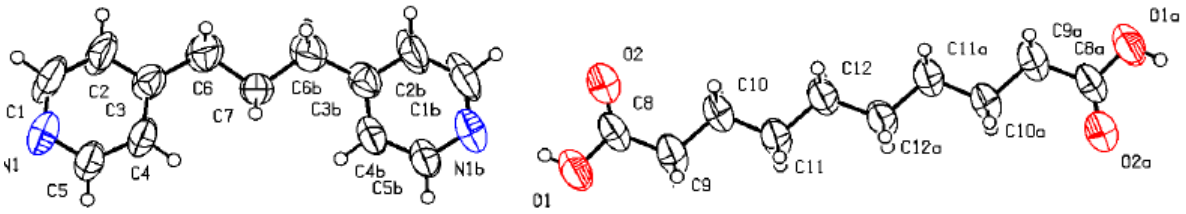

2·C10

ESI-XRAY Table 1. Crystal Data and Details of Measurements for compounds 1·C4 to 1·C10

compound	**Succinic acid**	**Glutaric acid**	**Adipic acid**	**Pimelic acid**	**Suberic acid**	**Azelaic acid**	**Sebacic acid**
	1C4	**1**C5	**1**C6	**1**C7	**1**C8	**1**C9	**1**C10
Formula	$C_{16}H_{18}N_2O_4$	$C_{17}H_{20}N_2O_4$	$C_{18}H_{22}N_2O_4$	$C_{19}H_{24}N_2O_4$	$C_{20}H_{26}N_2O_4$	$C_{21}H_{28}N_2O_4$	$C_{22}H_{28}N_2O_4$
M_r	302.32	316.35	330.38	344.40	358.43	372.45	384.46
system	Monoclinic	Monoclinic	Triclinic	Monoclinic	Monoclinic	Monoclinic	Triclinic
space group	C2/c	$P2_1/c$	P -1	$P2_1/c$	$P2_1/c$	C2/c	P-1
a [Å]	21.121(2)	12.2889(4)	7.2159(6)	11.138(1)	11.6701(5)	10.656(3)	6.9363(4)
b [Å]	4.9224(3)	11.1400(5)	7.3354(7)	47.332(5)	20.9348(7)	8.429(1)	6.9574(4)
c [Å]	16.6376(12)	24.3454(12)	8.8449(7)	14.436(2)	12.9988(5)	22.310(2)	12.0029(8)
α [°]	90.00	90.00	90.210(7)	90.00	90.00	90.00	77.230(5)
β [°]	119.752(6)	96.933(4)	93.428(6)	105.832(1)	114.656(5)	99.851(4)	73.739(6)
γ [°]	90.00	90.00	115.808(9)	90.00	90.00	90.00	71.192(6)
V [Å³]	1501.7(2)	3308.5(2)	420.49(6)	7322(1)	2886.2(2)	1974.3(6)	520.90(5)
Z	4	8	1	16	6	4	1
d_{calc}	1.337	1.270	1.305	1.250	1.137	1.253	1.226
F(000)	640	1344	176	2944	1152	800	206
$\mu(Mo_{K\alpha})$ [mm^{-1}]	0.097	0.091	0.093	0.088	0.086	0.087	0.084
θ_{max} [°]	29	28	29	28	28.4	25	29
measured reflns	3714	18988	4004	60898	13402	1768	4579
unique reflns	1728	7286	1907	16573	6159	1720	2332
refined parameters	104	427	112	934	365	127	144
GOF on F^2	0.954	0.900	0.916	0.986	1.035	1.006	0.862
*R*1 [on *F*, $I > 2\sigma(I)$]	0.0427	0.0827	0.0499	0.0827	0.0793	0.0424	0.0545
*wR*2(onF^2,all data)	0.1136	0.2049	0.1370	0.2987	0.2062	0.1291	0.1505

ESI-XRAY Table 2. Crystal Data and Details of Measurements for compounds **2**·C4 to **2**·C10

compound	**2C5**	**2C6**	**2C7**	**2C10**
Formula	$C_{18}H_{22}N_2O_4$	$C_{19}H_{24}N_2O_4$	$C_{20}H_{26}N_2O_4$	$C_{23}H_{32}N_2O_4$
M_r	330.38	344.4	358.43	400.51
system	Monoclinic	Monoclinic	Triclinic	Monoclinic
space group	$P2_1/c$	C2/c	P-1	C2/c
a [Å]	5.43048(2)	13.7629(8)	7.1246(4)	12.661(3)
b [Å]	20.7179(7)	5.3869(4)	11.1403(4)	10.129(1)
c [Å]	15.4813(6)	24.640(2)	12.9265(7)	17.361(2)
α [°]	90.00	90.00	81.099(4)	90
β [°]	92.205(3)	95.597(6)	84.868(5)	93.13(1)
γ [°]	90.00	90.00	71.717(4)	90
V [Å³]	1740.6(1)	1818.1(2)	961.54(8)	2223.1(6)
Z	4	4	2	4
d_{calc} [g mm^{-3}]	1.261	1.258	1.238	1.197
F(000)	704	736	384	864
$\mu(Mo_{K\alpha})$ [mm^{-1}]	0.090	0.089	0.086	0.082
θ_{max} [°]	26	25	26	25
measured reflns	15427	4312	7249	5603
unique reflns	3411	1586	3687	1935
refined parameters	239	114	243	132
GOF on F^2	1.159	1.099	0.911	1.023
*R*1 [on *F*, $I > 2\sigma(I)$]	0.0882	0.0647	0.0580	0.0934
*wR*2(onF^2,all data)	0.1685	0.1429	0.1333	0.2667

ESI-XRAY Table 3. Relevant hydrogen bonding distances (in Å) for all the compounds structurally characterized in this paper

compound	**1C4**	**1C5**	**1C6**	**1C7**	**1C8**	**1C9**	**1C10**
N···(H)O[a]	2.607(2)	2.650(4), 2.631(5) 2.656(5), 2.649(5)	2.613(2)	2.611(4), 2.642(4) 2.629(4), 2.633(4) 2.643(4)	2.645(3) 2.629(3) 2.620(3)	2.653(2)	2.654(2)
C(H)···O[b]	3.345(3)	3.295(6) 3.272(6)	3.330(2)	3.195(6), 3.294(6) 3.190(5), 3.250(5) 3.239(6), 3.245(5) 3.258(5)	3.336(4) 3.238(3) 3.437(4)	3.413(2)	3.355(3)
compound	**---**	**2C5**	**2C6**	**2C7**	**---**	**---**	**2C10**
N···(H)O[a]		2.624(3) 2.653(3)	2.676(3)	2.645(3) 2.644(3)			2.660(5)
C(H)···O[b]		3.321(4), 3.467(4) 3.334(4)	3.290(3)	3.269(3), 3.436(3) 3.346(3)			

a) N···O < 3.0 Å ; b) C···O < 3.5 Å

DIFFERENTIAL SCANNING CALORIMETRY (DSC)

Differential scanning calorimetry was used to measure the melting point of all compounds and to detect the presence of additional crystalline phases. In some cases solid-solid phase transitions to higher temperature polymorphs were also observed before melting (**1**·C6, 133 °C (onset), **1**·C8, 131 °C (onset), **1**·C9, 123 °C (onset).

Calorimetric measurements were performed using a Perkin Elmer Pyris Diamond DSC differential scanning calorimeter equipped with a model ULSP 90 intra-cooler. The instrument was calibrated with high-purity standards (indium and cyclohexane) at 5 K min^{-1}. The samples (2–4 mg) were placed in aluminium closed pans, and heating was carried out at 5°C min^{-1} .

ESI-DSC Table 1. Melting point (onset) values for all crystalline materials. All values are in °C.

---

mp(**1**C4) = 169.3	mp(**2**C4) = 155.8
mp(**1**C5) = 134.2	mp(**2**C5) = 131.3
mp(**1**C6) = 173.7	mp(**2**C6) = 112.6
mp(**1**C7) = 145.1	mp(**2**C7) = 138.1
mp(**1**C8) = 180.9	mp(**2**C8) = 110.8
mp(**1**C9) = 131.1	mp(**2**C9) = 131.1
mp(**1**C10) = 160.1	mp(**2**C10) = 101.1

Thermal behaviour - BPA

Differential scanning calorimetry measurements for **1**·C4, **1**·C5, **1**·C6, **1**·C7, **1**·C8, **1**·C9 and **1**·C10 adducts.

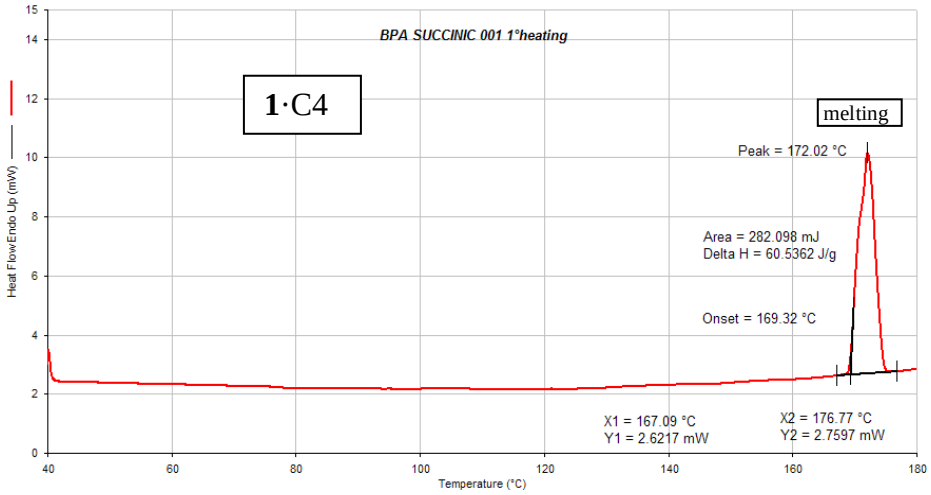

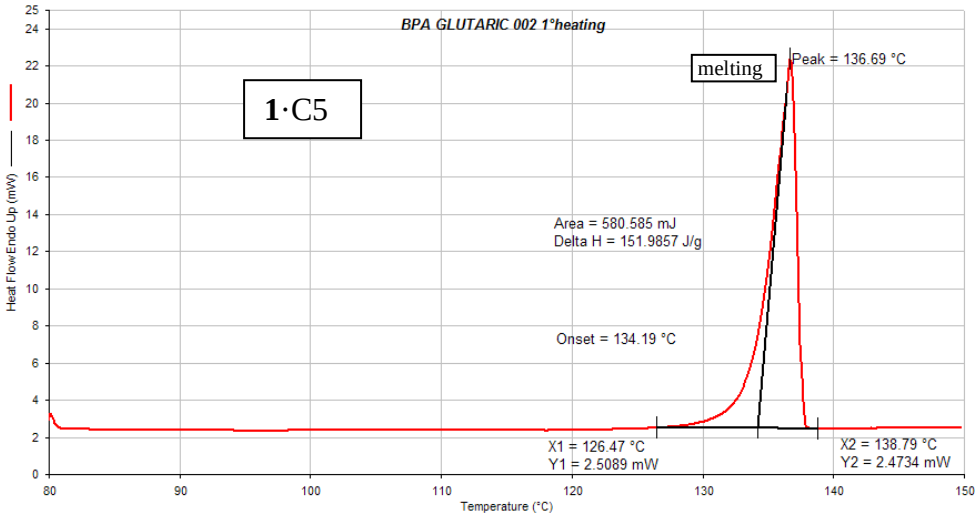
BPA GLUTARIC 002 1°heating
1·C5
melting
Peak = 136.69 °C
Area = 580.585 mJ
Delta H = 151.9857 J/g
Onset = 134.19 °C
X1 = 126.47 °C
Y1 = 2.5089 mW
X2 = 138.79 °C
Y2 = 2.4734 mW
Heat Flow Endo Up (mW)
Temperature (°C)

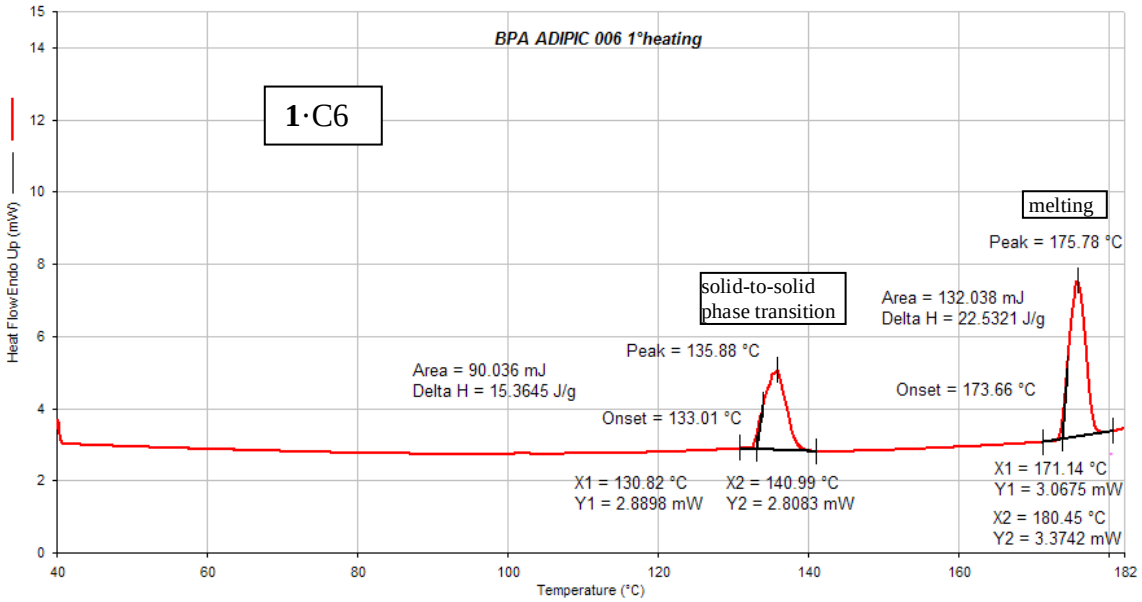
BPA ADIPIC 006 1°heating
1·C6
melting
Peak = 175.78 °C
solid-to-solid
phase transition
Area = 132.038 mJ
Delta H = 22.5321 J/g
Peak = 135.88 °C
Area = 90.036 mJ
Delta H = 15.3645 J/g
Onset = 173.66 °C
Onset = 133.01 °C
X1 = 171.14 °C
Y1 = 3.0675 mW
X2 = 180.45 °C
Y2 = 3.3742 mW
X1 = 130.82 °C
Y1 = 2.8898 mW
X2 = 140.99 °C
Y2 = 2.8083 mW
Heat Flow Endo Up (mW)
Temperature (°C)

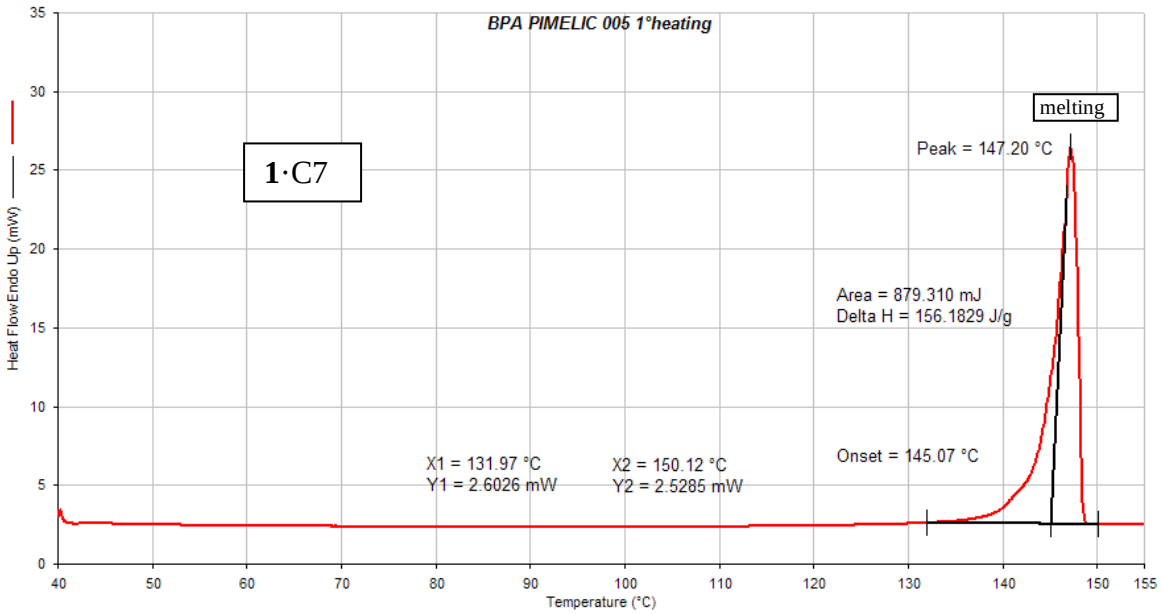
BPA PIMELIC 005 1°heating
1·C7
melting
Peak = 147.20 °C
Area = 879.310 mJ
Delta H = 156.1829 J/g
Onset = 145.07 °C
X1 = 131.97 °C
Y1 = 2.6026 mW
X2 = 150.12 °C
Y2 = 2.5285 mW
Heat Flow Endo Up (mW)
Temperature (°C)

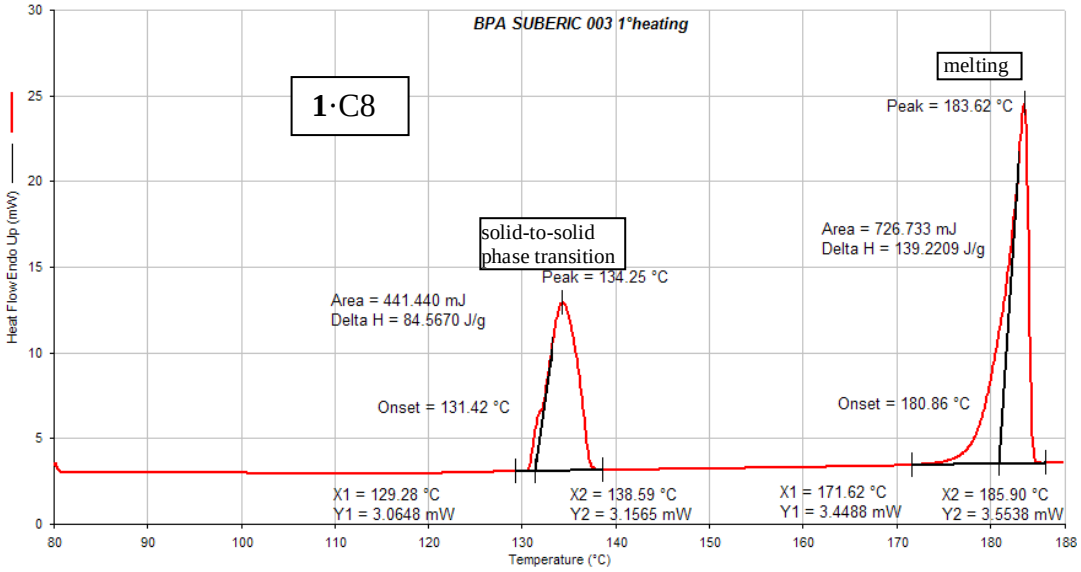

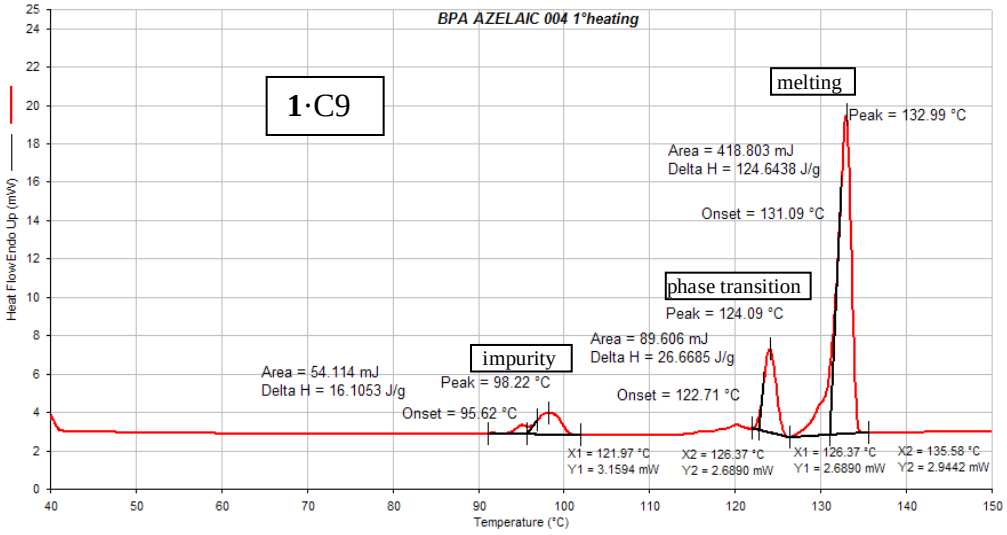

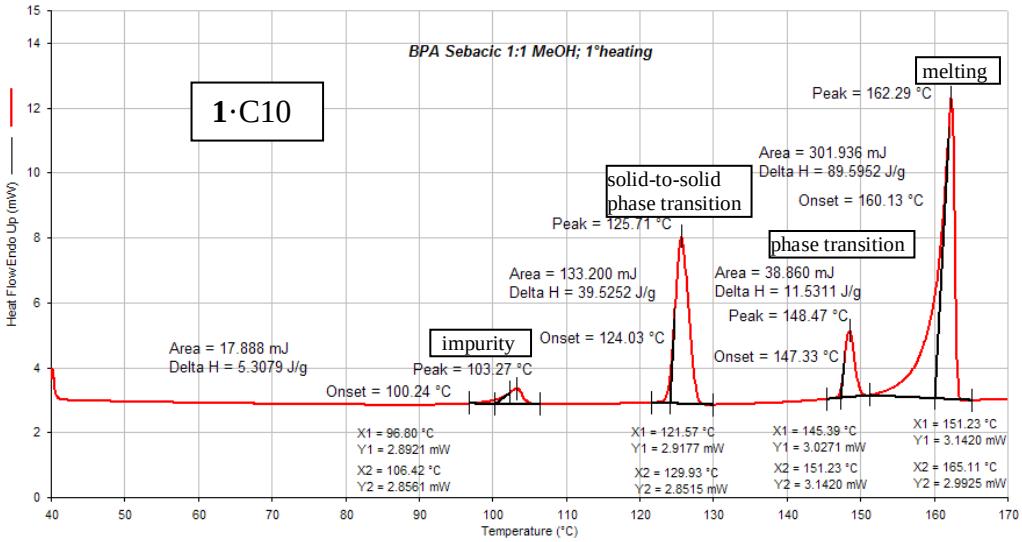

Thermal behaviour – BPP

Differential scanning calorimetry measurements for 2·C4, 2·C5, 2·C6, 2·C7, 2·C8, 2·C9 and 2·C10 adducts.

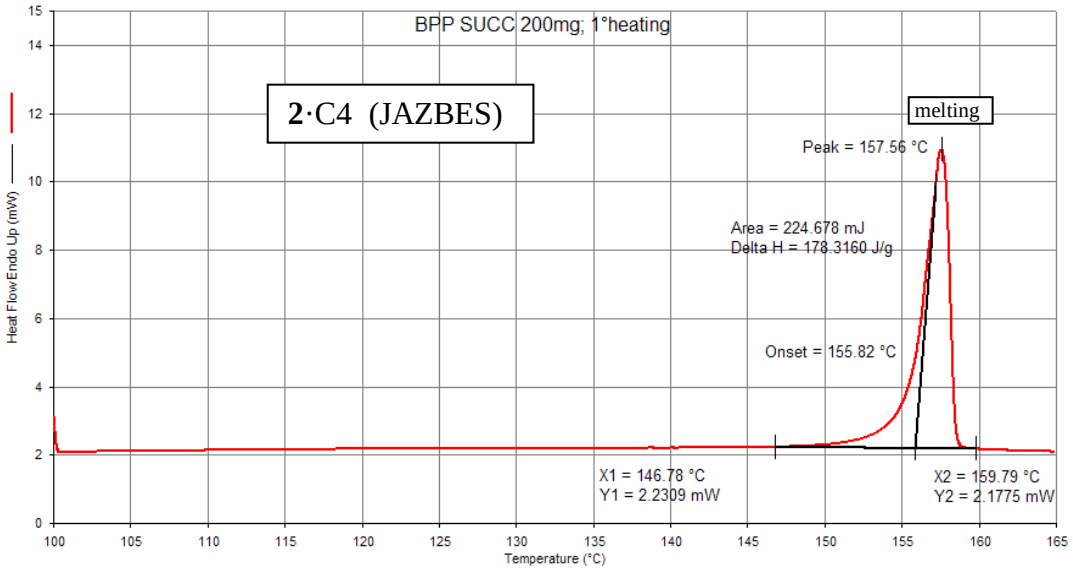

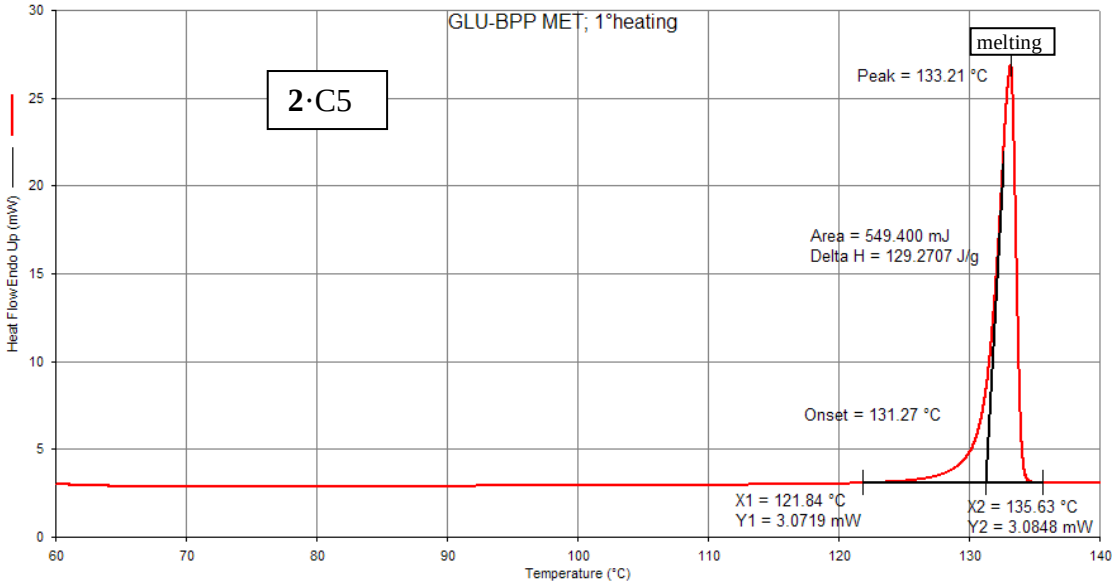

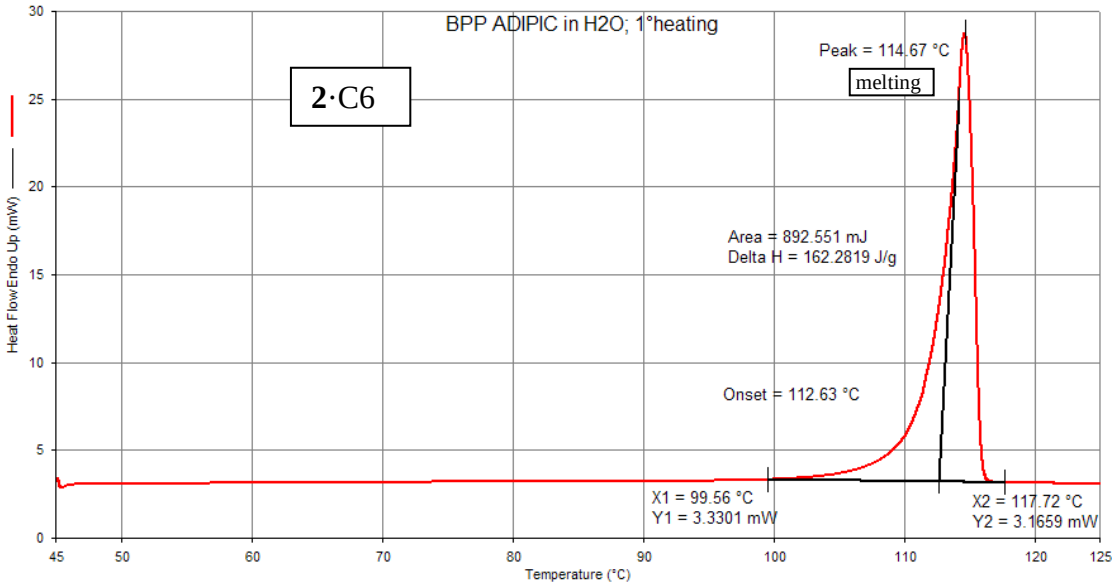

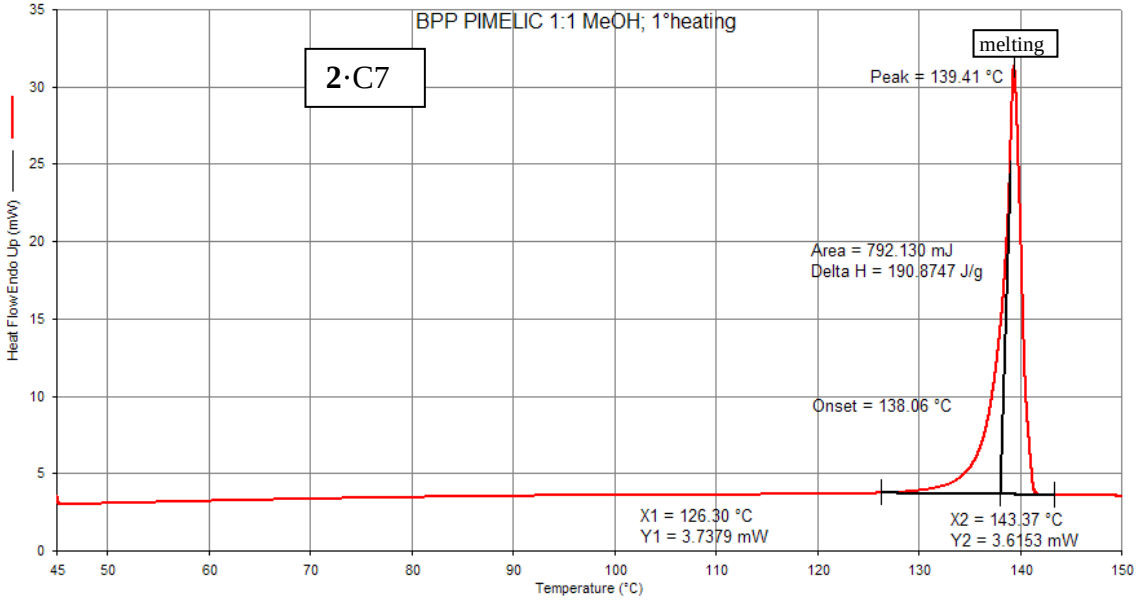
BPP PIMELIC 1:1 MeOH; 1°heating
2·C7
melting
Peak = 139.41 °C
Area = 792.130 mJ
Delta H = 190.8747 J/g
Onset = 138.06 °C
X1 = 126.30 °C
Y1 = 3.7379 mW
X2 = 143.37 °C
Y2 = 3.6153 mW
Heat Flow Endo Up (mW)
Temperature (°C)

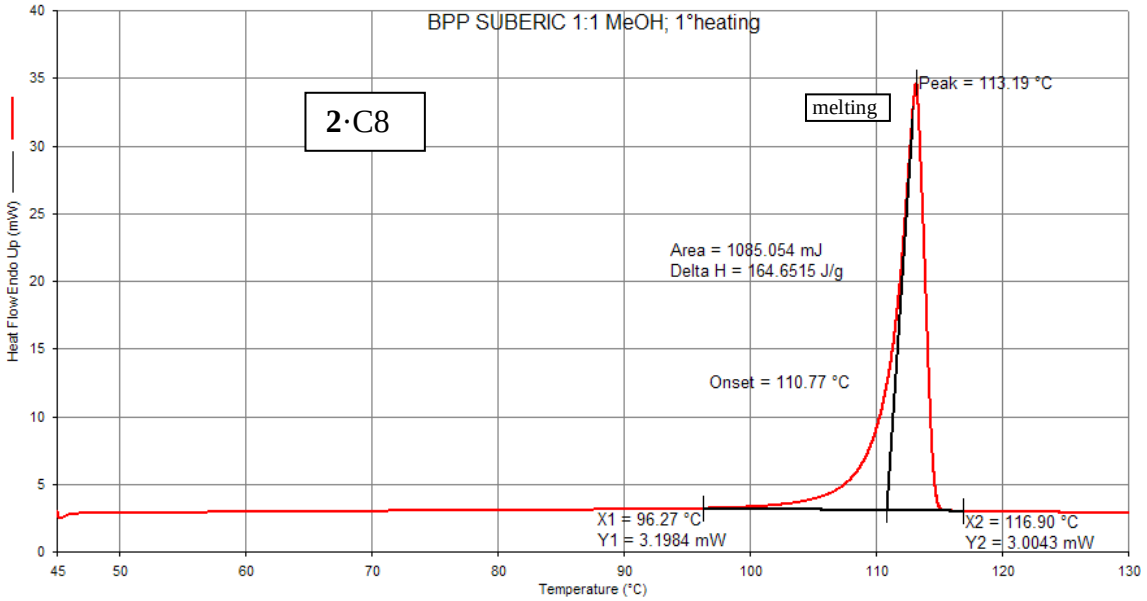
BPP SUBERIC 1:1 MeOH; 1°heating
2·C8
melting
Peak = 113.19 °C
Area = 1085.054 mJ
Delta H = 164.6515 J/g
Onset = 110.77 °C
X1 = 96.27 °C
Y1 = 3.1984 mW
X2 = 116.90 °C
Y2 = 3.0043 mW
Heat Flow Endo Up (mW)
Temperature (°C)

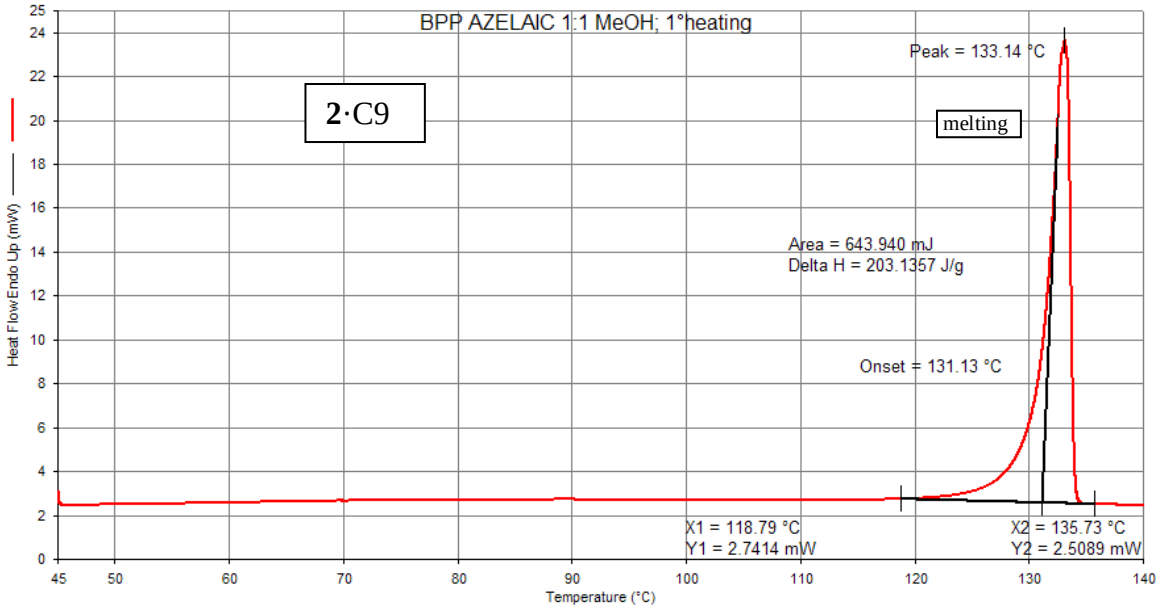
BPP AZELAIC 1:1 MeOH; 1°heating
2·C9
Peak = 133.14 °C
melting
Area = 643.940 mJ
Delta H = 203.1357 J/g
Onset = 131.13 °C
X1 = 118.79 °C
Y1 = 2.7414 mW
X2 = 135.73 °C
Y2 = 2.5089 mW
Heat Flow Endo Up (mW)
Temperature (°C)

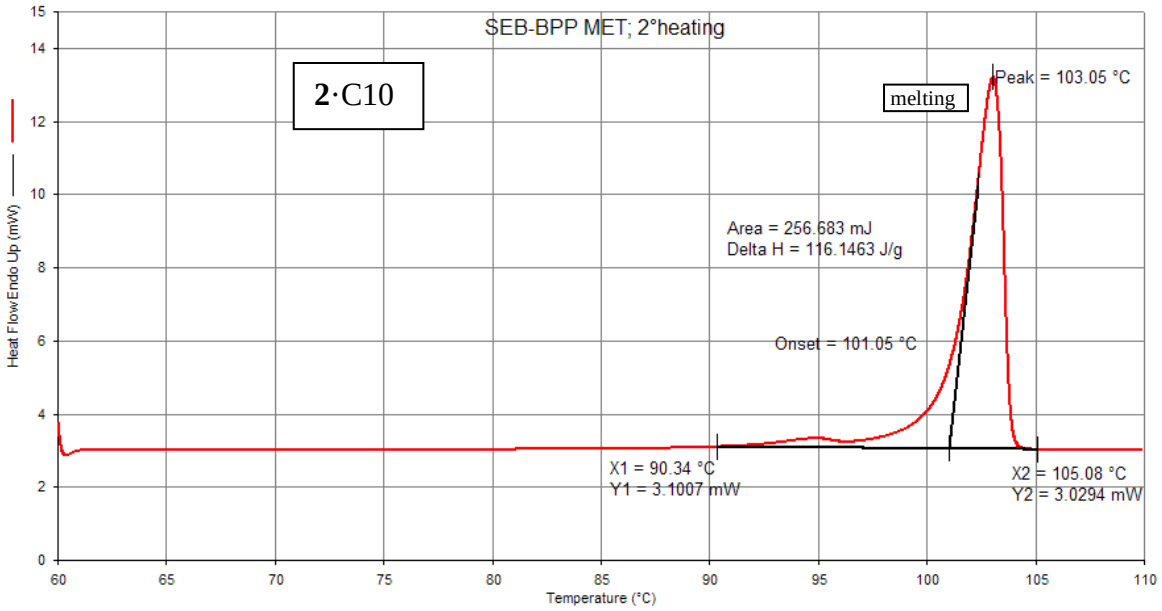
SEB-BPP MET; 2°heating
2·C10
melting
Peak = 103.05 °C
Area = 256.683 mJ
Delta H = 116.1463 J/g
Onset = 101.05 °C
X1 = 90.34 °C
Y1 = 3.1007 mW
X2 = 105.08 °C
Y2 = 3.0294 mW
Heat Flow Endo Up (mW)
Temperature (°C)
0
2
4
6
8
10
12
14
15
60
65
70
75
80
85
90
95
100
105
110

XRPD Patterns - BPA:acid

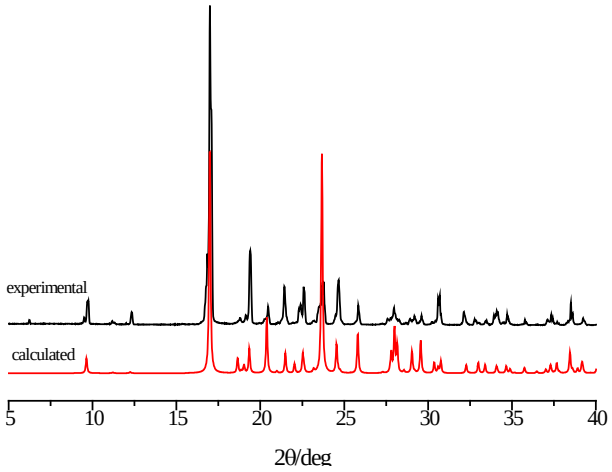

ESI-XRPD Figure 1. Calculated (red) and experimental (black) XRPD patterns for 1·C4

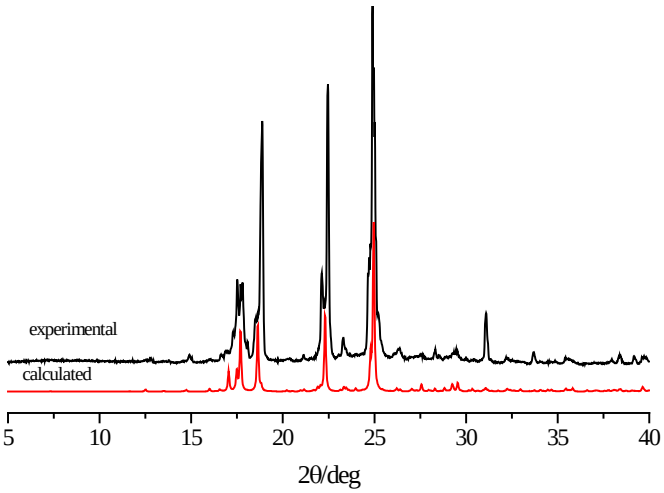

ESI-XRPD Figure 2. Calculated (red) and experimental (black) XRPD patterns for 1·C5

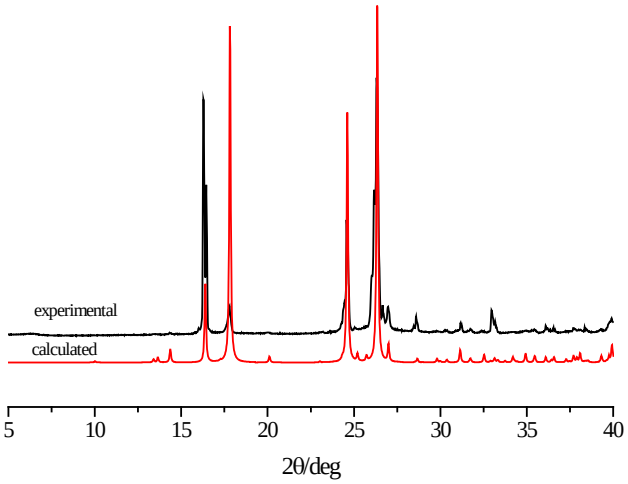

ESI-XRPD Figure 3. Calculated (red) and experimental (black) XRPD patterns for 1·C6

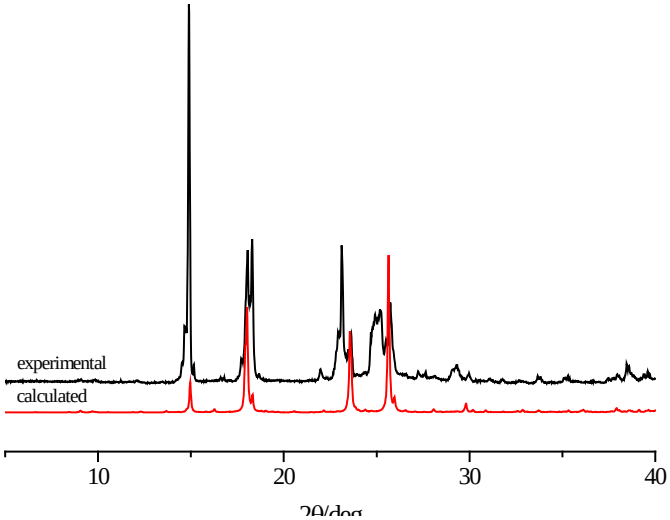

ESI-XRPD Figure 4. Calculated (red) and experimental (black) XRPD patterns for 1·C7

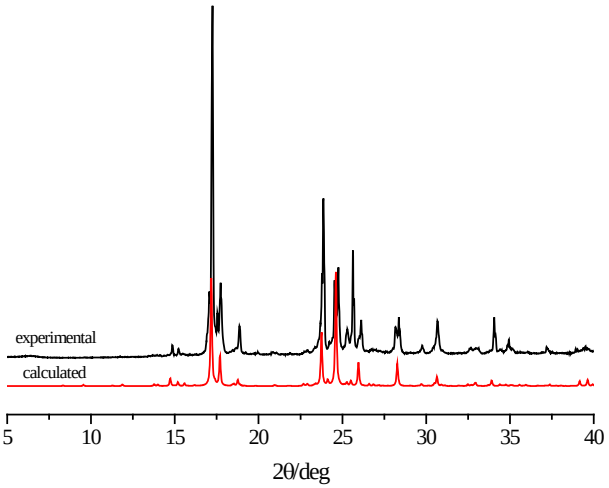

ESI-XRPD Figure 5. Calculated (red) and experimental (black) XRPD patterns for 1·C8

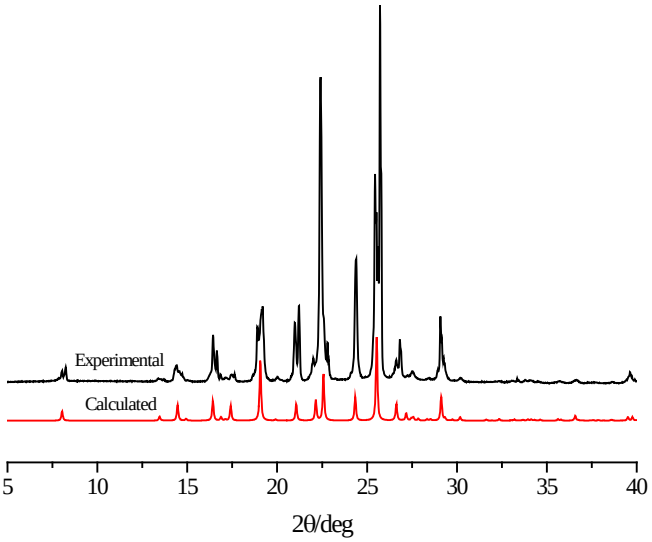

ESI-XRPD Figure 6. Calculated (red) and experimental (black) XRPD patterns for 1·C9

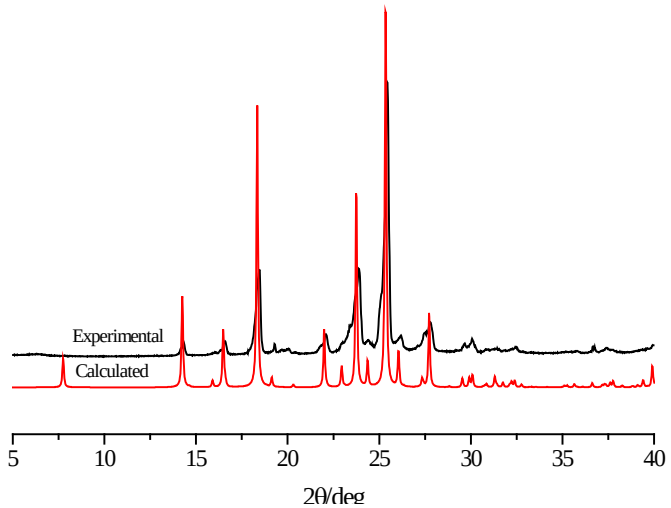

ESI-XRPD Figure 7. Calculated (red) and experimental (black) XRPD patterns for 1·C10

XRPD Patterns - BPP:acid

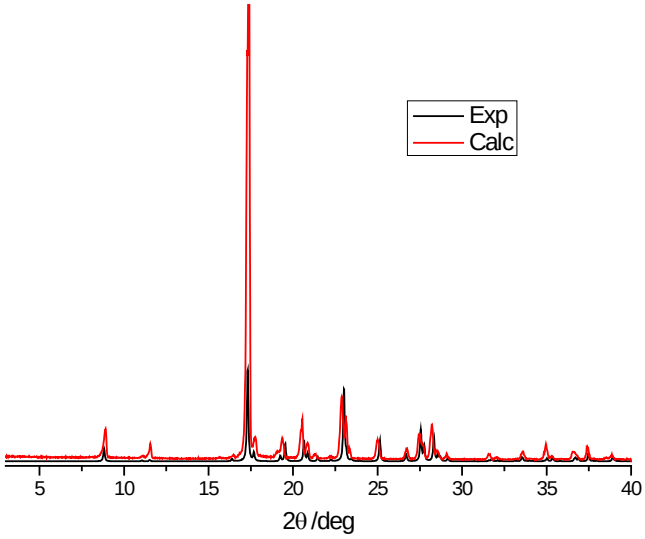

ESI-XRPD Figure 8. Calculated (red) and experimental (black) XRPD patterns for 2·C4 (CSD refcode calc = JAZBES)

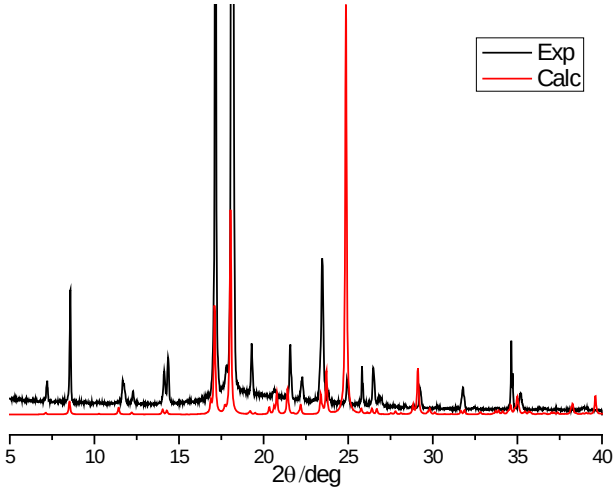

ESI-XRPD Figure 9. Calculated (red) and experimental (black) XRPD patterns for 2·C5

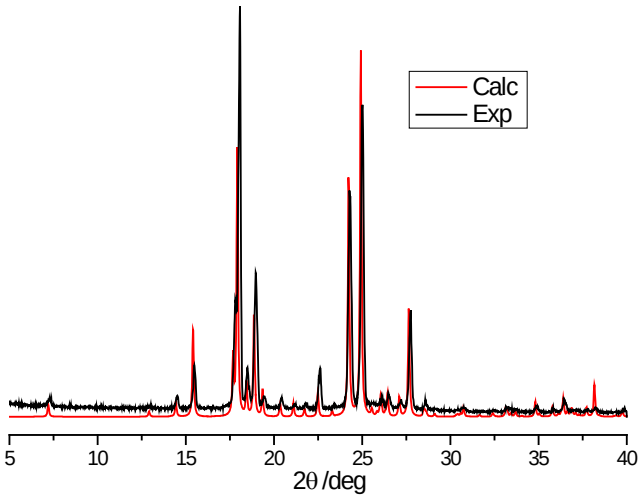

ESI-XRPD Figure 10. Calculated (red) and experimental (black) XRPD patterns for 2·C6

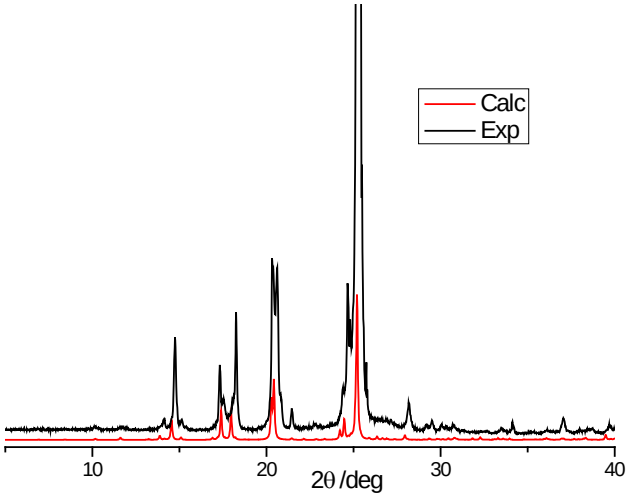

ESI-XRPD Figure 11. Calculated (red) and experimental (black) XRPD patterns for 2·C7

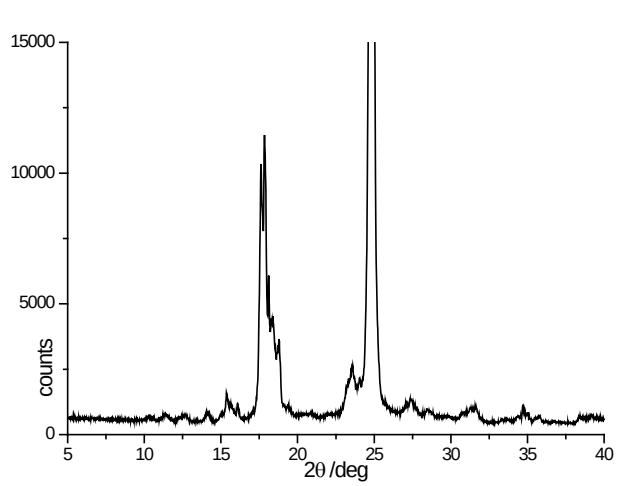

ESI-XRPD Figure 12. Experimental XRPD pattern for 2·C8

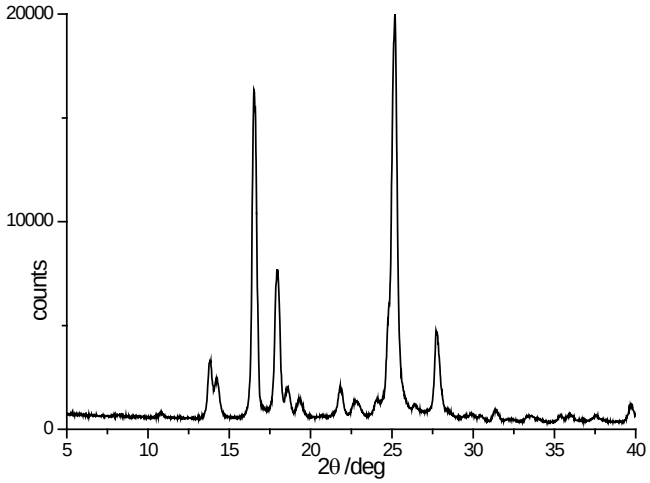

ESI-XRPD Figure 13. Experimental XRPD patterns for 2·C9

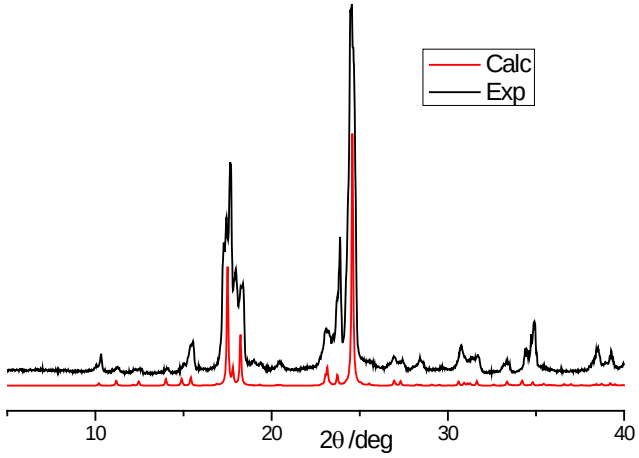

ESI-XRPD Figure 14. Calculated (red) and experimental (black) XRPD patterns for 2·C10

Solid-state NMR

All NMR measurements were recorded on a Bruker Avance II 400 spectrometer operating at 400.23, 100.65 and 40.55 MHz for ^{1}H, ^{13}C and ^{15}N, respectively. ^{13}C and ^{15}N spectra were recorded with a 4 mm probe at the spinning speed of 12 kHz. A ramp CP pulse sequence with a TPPM decoupling was used with a contact time of 3 (^{13}C) or 4 ms (^{15}N), a ^{1}H 90° pulse of 3.35 μs, recycle delays of 15–40 s and about 128 and 3000 transients for the ^{13}C and ^{15}N spectra, respectively. 1D and 2D ^{1}H DQ MAS experiments were performed on a 2.5 mm Bruker probe at the spinning speed of 32 kHz. The ^{1}H MAS spectra were acquired with the DEPTH sequence ($\pi/2–\pi–\pi$) for suppressing the probe background signal. The back-to-back (BABA) recoupling pulse sequence, which efficiently generates DQ coherences in the presence of very fast MAS, was used to acquire 2D ^{1}H DQ MAS NMR spectra with excitation times of one rotor period. For all samples, the ^{1}H 90° pulse length was 3.25 ms, and a recycle delay of 15-40 s was used. For each of 64 increments of t_1, 128 transients were averaged. ^{1}H, ^{13}C and ^{15}N chemical shifts were referenced via the resonance of solids adamantate (^{1}H signal at 1.87 ppm), HMB (^{13}C methyl signal at 17.4 ppm) and $(NH_4)_2SO_4$ (^{15}N signal at -355.8 ppm with respect to CH_3NO_2).

ESI-NMR Table 1: ^{13}C and ^{15}N chemical shift data (ppm) of the acid-BPA and acid-BPP series together with signal integral values (between brackets) and main O-N X-ray distances (Å).

	BPA			BPP		
Acid	**^{13}C**	**^{15}N**	**O-N**	**^{13}C**	**^{15}N**	**O-N**
Succinic	176.1	249.7	2.607(2)			2.604
Glutaric	175.8 (2) 173.9 (1)	258.1 253.5 251.5	2.631 (5) 2.649 (5) 2.650(5) 2.656 (5)	176.1	253.9	2.624 (3) 2.653 (3)
Adipic	175.9	248.4	2.613 (2)	177.9	261.2	2.676 (3)
Pimelic	176.2	257.1 255.6 253.6	2.642 (4) 2.629 (4) 2.633 (2) 2.643 (2) 2.611 (4)	175.9	253.5	2.645 (3) 2.644 (3)
Suberic	177.2 (2) 177.8 (1)	252.3 (1.7) 253.7 (1)	2.645 (3) 2.629 (3) 2.620 (3)	175.9 175.2 sh	252.5	No X-ray
Azelaic	177.3	255.7	2.653 (2)	176.1	251.5	No X-ray
Sebacic	177.2	255.1	2.654 (2)	177.0 (2.2) 175.9 (1)	261.4 254.2	2.660(5)

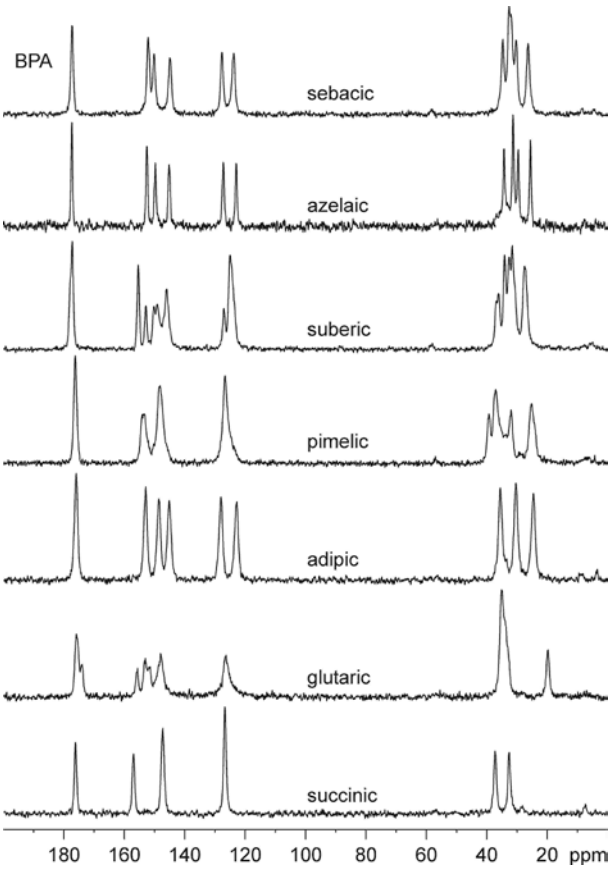

ESI-NMR Figure 1: ^{13}C CPMAS NMR spectra of the acid-BPA series recorded with a spinning speed of 12 kHz.

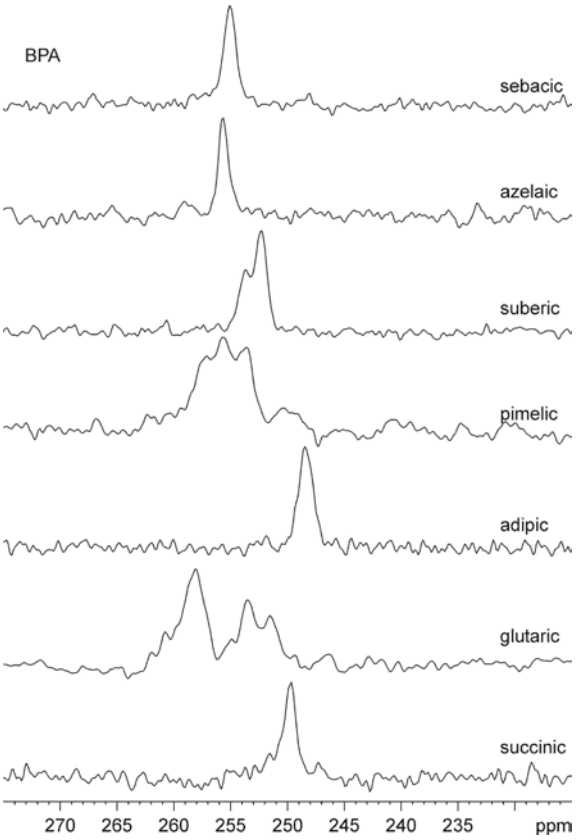

ESI-NMR Figure 2: ^{15}N CPMAS NMR spectra of the acid-BPA series recorded with a spinning speed of 6 kHz.

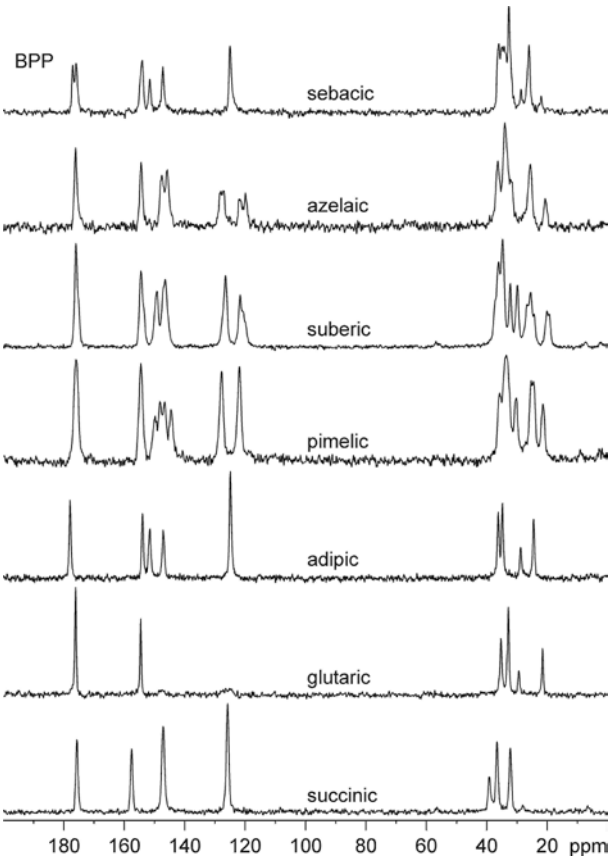

ESI-NMR Figure 3: ^{13}C CPMAS NMR spectra of the acid-BPP series recorded with a spinning speed of 12 kHz.

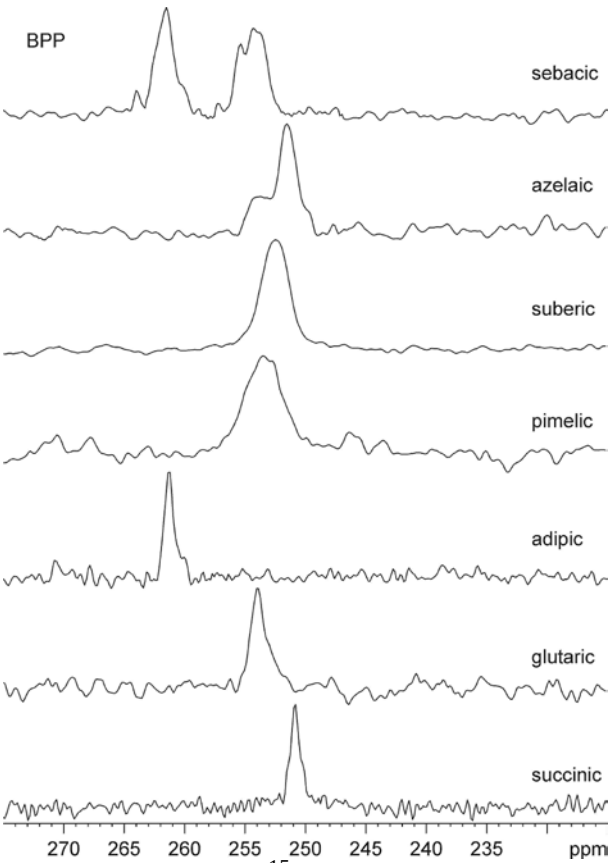

ESI-NMR Figure 4: ^{15}N CPMAS NMR spectra of the acid-BPP series recorded with a spinning speed of 6 kHz.

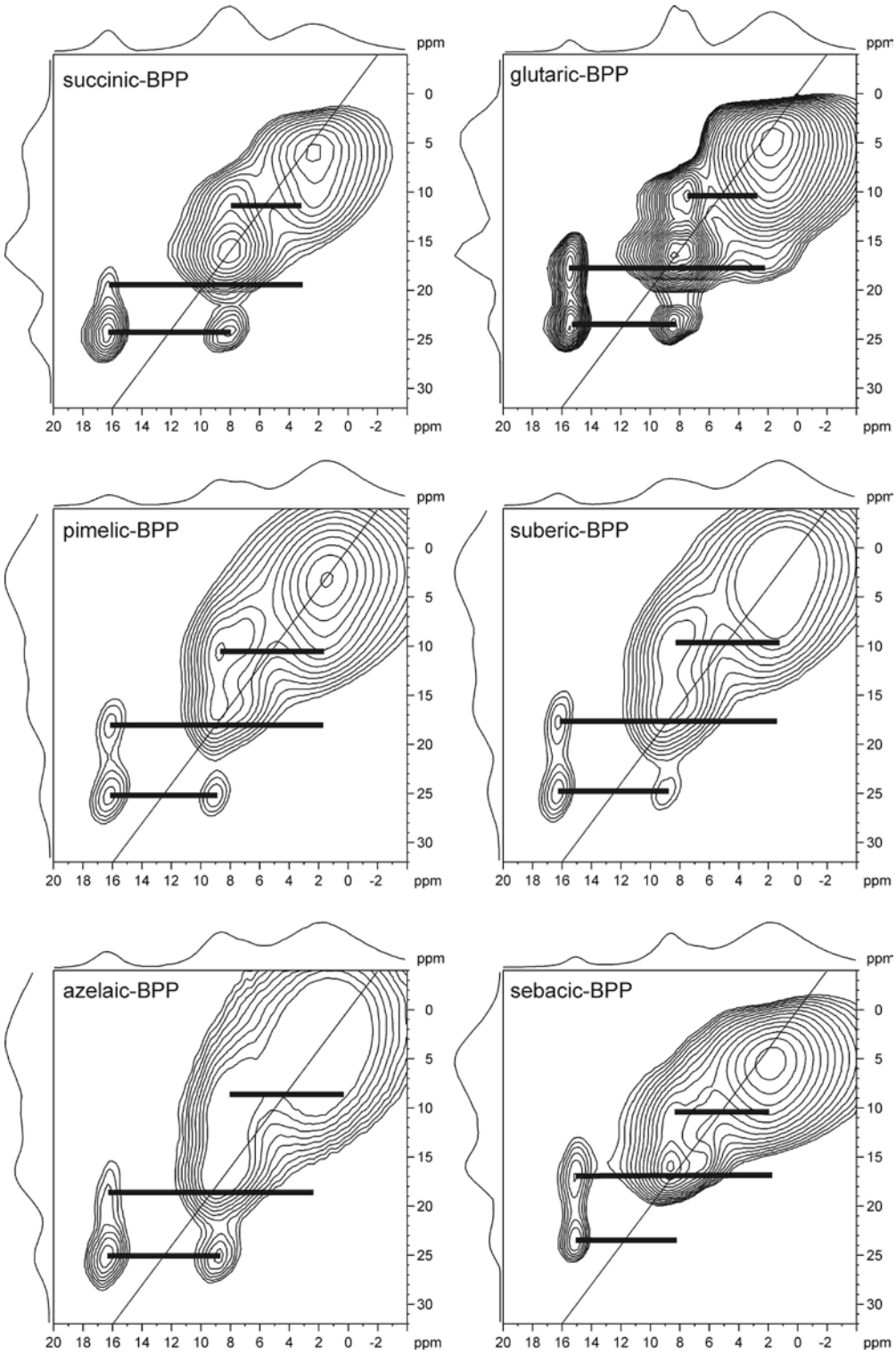

ESI-NMR Figure 5: ^{1}H 2D DQ MAS NMR spectra of the acid-BPP series (adipic-BPP not reported) recorded with a spinning speed of 32 kHz.

The presence of a correlation between hydrogen-bonded signals (around 15-16 ppm) and aromatic signals (around 7-8 ppm) in all spectra confirm the proximity between these two types of hydrogen atoms and thus the formation of acid-base adducts through O-H···N interactions. Furthermore, similarities of all the other correlations in all spectra allow to role out the presence of different crystal packing for the suberic-BPP and azelaic-BPP adducts whose X-ray structures are not available.